AN ABSTRACT OF THE THESIS OF

Antoine Renaud Fabrice Badan-Dangon for the Master of Science
(Name of student) (Degree)

degree in Oceanography presented on January 13, 1975
(Major Department) (Date)

Title: DENSITY CURRENTS INDUCED BY FREEZING IN A SHALLOW POLAR OCEAN: SOME HEURISTIC MODELS

Abstract approved: Redacted for privacy
(Dr. Stephen Neshyba)

An ice cover which progrades over a shallow ocean in the form of an ice front may induce a baroclinic flow in the underlying water, provided that the brine excluded from the freezing surface layer is mixed rapidly through out the underlying water column. A series of models are developed to gain insight into the significance of this process in an initially motionless ocean and of its interaction with a pre-established circulation. For a simplified case, the near-surface flow rate is of the order of 2 cm $sec^{-1}$ and directed to the east in the northern Hemisphere. The volume transport under the ice front and assuming a typical depth of 100 m, is about 0.1 Sverdrup. However, for the case of an interaction with pre-existing circulation, and in particular with a circular motion, higher speeds of the induced currents may be expected. It might be concluded that the process may play a significant role in winter circulation in shallow marginal polar seas, where a winter pycnocline is absent.

# Density Currents Induced by Freezing in a Shallow Polar Ocean: Some Heuristic Models

by

Antoine Renaud Fabrice Badan-Dangon

A THESIS

submitted to

Oregon State University

in partial fulfillment of
the requirements for the
degree of

Master of Science

Completed January 1975

Commencement June 1975

APPROVED:

Redacted for privacy

Associate Professor of Oceanography
in charge of major

Redacted for privacy

Dean of School of Oceanography

Redacted for privacy

Dean of Graduate School

Date thesis is presented January 13, 1975

Typed by Mary Jo Stratton for Antoine Renaud Fabrice Badan-Dangon

## ACKNOWLEDGEMENTS

I am indebted to Dr. Stephen Neshyba for his guidance and encouragements have made this thesis possible.

My first year of graduate work was supervised by Dr. William P. Elliott, who spent many hours sharing not only cigars and cups of tea, but precious advice and concern. His philosophy and kindness will always be gratefully remembered.

Many people have read this manuscript and contributed numerous, helpful comments. Besides the members of my committee, Drs. Charles Miller and James McCauley are to be especially thanked for their criticism.

Support for my graduate work was provided by the Consejo Nacional de Ciencia y Tecnologia of Mexico.


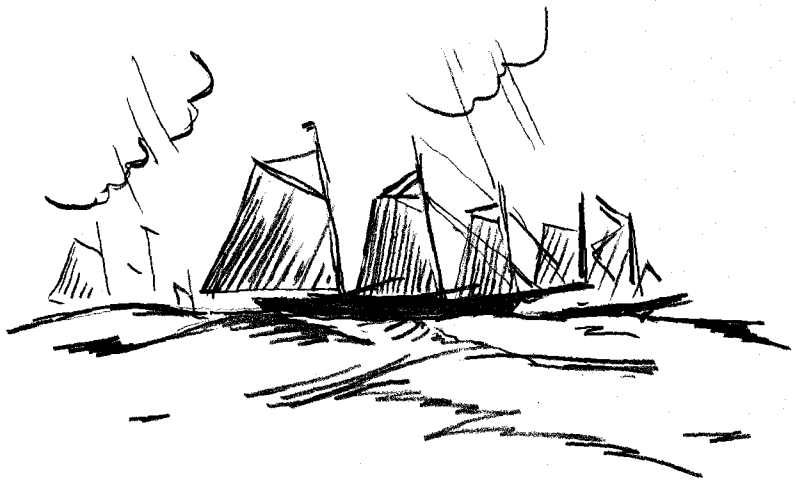

TABLE OF CONTENTS


| | Page |
|---|---|
| I. INTRODUCTION | 1 |
| II. THE BASIC MODEL | 6 |
| A. Density Changes in the Underlying Fluid | 8 |
| B. The Resulting Pressure Field | 11 |
| C. Relative Current and Transport under the Freezing Zone | 13 |
| D. Transport as Function of the Geometry of the System | 14 |
| E. Limitations of the Basic Model | 19 |
| III. THE ADVECTION MODEL: RECTILINEAR MOTION | 20 |
| A. Description of the Model | 21 |
| B. Three Possibilities | 22 |
| IV. CIRCULAR MOTION | 31 |
| V. DISCUSSION | 38 |
| A. Application to the Bering Sea Shelf | 41 |
| VI. EPILOGUE | 46 |
| BIBLIOGRAPHY | 48 |

# LIST OF FIGURES


| Figure | | Page |
|---|---|---|
| 1 | The basic model and the reference system. | 7 |
| 2 | Schematic model of a southward prograding ice front in a shallow marginal polar sea. | 9 |
| 3 | A vertically magnified diagram of the slope of the 1 db pressure surface in the shallow marginal polar sea model. | 15 |
| 4 | Schematic model of an initially well mixed, shallow ocean in which a surface layer, h, is to be frozen. | 16 |
| 5 | Evolution of the system for the case [(C-U) = 0]. [Case A]. | 23 |
| 6 | Evolution of the system for the case [(C-U) < 0]. [Case B]. | 26 |
| 7 | Evolution of the system for the case [(C-U) > 0]. [Case C]. | 28 |
| 8 | The flow regime for the three cases. | 29 |
| 9 | Interaction of the ice front with a gyre. | 32 |
| 10 | Density distribution resulting from the interaction of the ice front with a gyre. | 35 |
| 11 | The resulting flow regime. | 37 |
| 12 | The Bering Sea shelf. | 42 |
| 13 | The Bering Sea circulation according to Arsen'ev (1967). | 45 |
| 14 | Proposed scheme of ice front interaction with the existing circulation in the Bering Sea at two given points in time, t and $\Delta t$. | 45 |

# DENSITY CURRENTS INDUCED BY FREEZING IN A SHALLOW POLAR OCEAN: SOME HEURISTIC MODELS

## I. INTRODUCTION

In the polar regions the three phases of water, gaseous, liquid, and solid, interact on a grandiose scale which is not found anywhere else on earth. On the outer boundaries where the ice borders upon warmer waters of lower latitudes, the water constantly converts from one phase to another through processes that imply enormous amounts of heat being released or absorbed in an annual cycle (Zubov, 1945; Defant, 1961). One of the processes is the formation of sea ice which accounts for nearly two thirds of the world's mean ice cover (Maykut and Untersteiner, 1971).

The formation of sea ice is a much studied phenomenon. Zubov (1945) has provided an excellent review of the process of ice formation and ice types in polar seas. The problem of determining the freezing point of sea water has been analyzed most recently by Fujino et al. (1974) in the salinity range from 18.0‰ to 35.0‰ at pressures up to 100 bars. Doherty and Kester (1974), obtained an expression for the freezing point $T_f$ for salinities between 3.8‰ and 40.2‰ and depths from 0 to 500 m, if the principle of constancy of relative proportions of sea water constituents holds. Kester (1974) compared these two sets of results.

In the area of ice growth processes, Simpson (1958) has treated the problem of long range forecasting of ice conditions in an ocean with relatively constant salinity and density conditions. Similarly, Kolesnikov (1958), presented an approximate solution to the problem of ice growth, formulated theoretically. Tabata (1958) also dealt with the same ice growth aspect, but with a specific application to the Okhotsk Sea.

Recently also, Maykut and Untersteiner (1971) have developed a time-dependent thermodynamic model of the formation of sea ice. The relationship between ice cover and circulation has been examined in several recent papers. Foldvik and Kvinge (1974), discussed a thermohaline convection mechanism based on the depression of the freezing point of sea water with increasing pressure, providing an example of conditional instability of sea water at the freezing point. Lake and Lewis (1972) described salinity, temperature and currents beneath growing sea ice and showed the development of an isothermal, isohaline layer immediately below the ice cover. However, these data were taken in an arctic bay in which considerable summer melt runoff had diluted the surface waters. For all this, adequate field data describing open ocean freeze-up are still unavailable.

It is sufficient here to say that during the growth of a sheet of sea ice, salt is rejected into the underlying water due to the formation of pure ice crystals. Usually the loss of heat that permits the

formation of the sea ice is to the atmosphere. The ice crystals form a matrix in a layer at the top of the fluid, mechanically trapping some portion of the resulting brine. This accounts for the salinity of the sea ice. The remaining salts are released into the water layer immediately below the forming ice, causing it to be of higher density than the underlying water and leading to the onset of convective currents. This process has been studied theoretically and in the laboratory by Foster (1968a, 1968b). On the microscale, the salt exclusion produces unstable Rayleigh convection and on a much larger scale the effect is to increase the density of the mixed layer. This results in a modified distribution of mass which has been the subject of investigations by several different approaches.

Zubov (1943) has given a simple technique for the prediction of the depth of convective circulation based on considerations of the available potential energy of the system. More recently, Kraus and Turner (1967) provided a model of the seasonal thermocline in a non-freezing open ocean, based on conservation of the potential energy in a fluid column with convective mixing. Solomon (1969) considered these two models in a study of the large scale response of a two-layered Arctic Ocean to the sea ice formation. He concluded that neither model could be fully accepted. Lewis and Walker (1970) conducted a study on the water structure under a growing ice sheet with conditions of very small advective currents. Although

their reported density values are not accurate enough to allow a comparison between Zubov and Kraus-Turner models, they concluded that the water column undergoes changes that are imposed mainly by convective processes. Water motion beneath sea ice due to salt rejection at the freezing interface was reviewed by Lewis (1973).

Solomon (1969) studied the case of a two-layered ocean where, following the Kraus-Turner model, the bottom layer is eroded by vertical convective currents and a strong pycnocline is maintained between the layers. He concluded that a large scale horizontal density gradient is set up, producing a circulation. His model shows the resulting circulation to be weak with its vertical ageostrophic components strongly constrained by rotation. The motion is reported as having little oceanographic importance. The erosion of the pycnocline by convective processes mixes salt from the bottom layer upward into the top layer, thus offsetting the effect of the downward mixing of excluded salts and diminishing the resulting circulation.

In shallow polar oceans a pycnocline may be absent and, therefore, the mixed layer is the only layer present. From this and the above, a question arises: what is the importance of the mass distribution resulting from the formation of sea ice in a shallow ocean? In view of the large extent of shallow polar seas, particularly in the Arctic, it is here hypothesized that such a process may result

in appreciable currents and hence mass transport during the season of sea ice formation. Furthermore, if that be the case, such currents must interact with a pre-existing circulation in a way that may have important oceanographic consequences.

A theoretical analysis of this hypothesis is the objective for this research. In the sections that follow, a series of simple models are developed in order to demonstrate the importance of the induced density currents.

# II. THE BASIC MODEL

The basic model describes the mass and energy distribution processes that occur under a prograding ice front in a shallow, marginal arctic ocean. The concept of a marginal ocean here is taken to be one that borders at high latitudes with fully developed polar conditions and at lower latitudes with warmer waters, thus undergoing an annual cycle of sea ice formation and melting.

Suppose an annual southerly progradation of the ice front of the order of 1000 km occurs in a time span of three months. The mean progression rate is then of the order of 10 cm $sec^{-1}$. The concept of a prograding front is based on the fact that freezing does not take place simultaneously over the entire span of the order of 6° of latitude. This assumption is supported by ERTS Satellite photographs of the Bering Sea. Rather, there must be an active zone of freezing which is itself prograding.

The following simplifying assumptions are made:

(1) the freezing zone extends over one degree of latitude, or approximately 100 km.

(2) the ice thickness at the trailing edge of the front is of the order of 1 m.

(3) the freezing rate in the region behind the trailing edge of the front is negligible.

(4) the ice thickness increases linearly from leading to trailing edge of the front

(5) the sea has a uniform depth of 101 m and is initially motionless.

The model refers to a right hand coordinate system, with the positive X axis oriented to the east, the positive Y axis oriented to the north and the positive Z upwards. The reference system will be considered to be at rest with respect to the bottom. (Fig. 1). This model will be restricted to the effects of the thermodynamic processes that occur between the ocean and the atmosphere on the underlying water during the season of freeze-up. No consideration will be made of the effect of the wind stress at the surface. Other meteorological phenomena will be considered to be of such a scale as to have only a general effect on the model as a whole. Therefore,

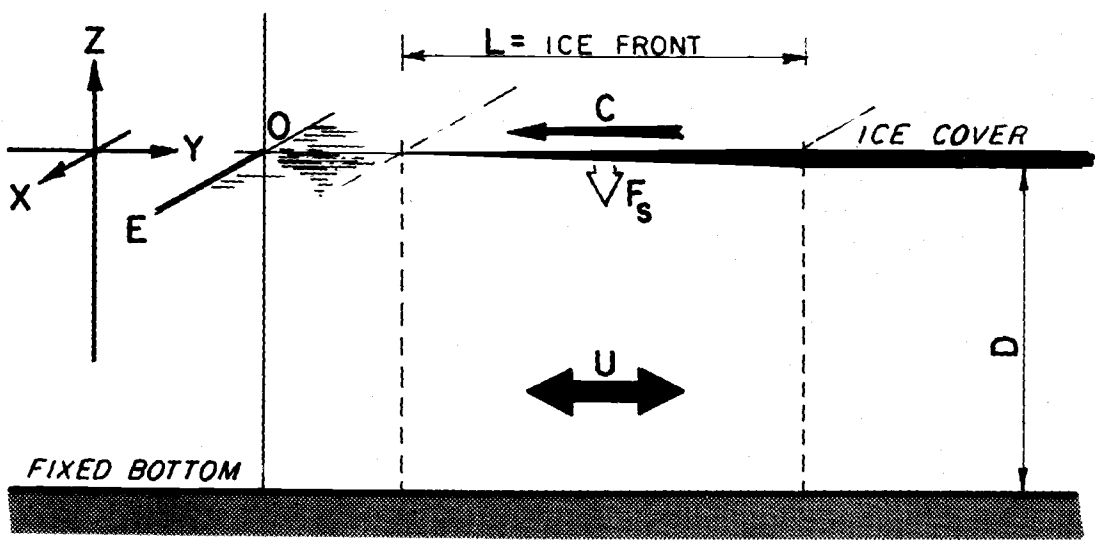


Fig. 1. The basic model and the reference system.

no variations in the properties of the atmosphere will be considered other than the presence of low air temperatures as a mechanism of heat absorption from the surface of the sea.

A. Density changes in the underlying fluid.

Figure 2 illustrates the ice front and the underlying fluid. Three zones are identified:

Zone A. The fluid immediately ahead of the ice front is taken to be vertically well mixed as a result of the surface cooling $Q_a$, and of convective mixing over the water column. The salinity $S_o$, of this fluid is taken to be 35.0‰. From Sverdrup et al., (1942) the freezing point depression is approximated by

$$\Delta\theta = - 0.0524\ S‰ \qquad (1)$$

from which one obtains a temperature $T_o = -1.834$ °C. From sigma-t tables, $\sigma_t$ is given as 28.1994, that is, $\rho_o = 1.0281994$.

Zone B. The active freezing zone is assumed to have everywhere a constant heat loss rate of $Q_B$, with a concomitant linearly increasing ice thickness in the northerly direction. The time for the progradation of the freezing zone past a given latitude is $10^6$ sec or about 12 days. It can be assumed that brine excluded from the freezing layer mixes rapidly with the underlying fluid. Where the salt flux at the ice-water interface is constant, Foster (1968), showed

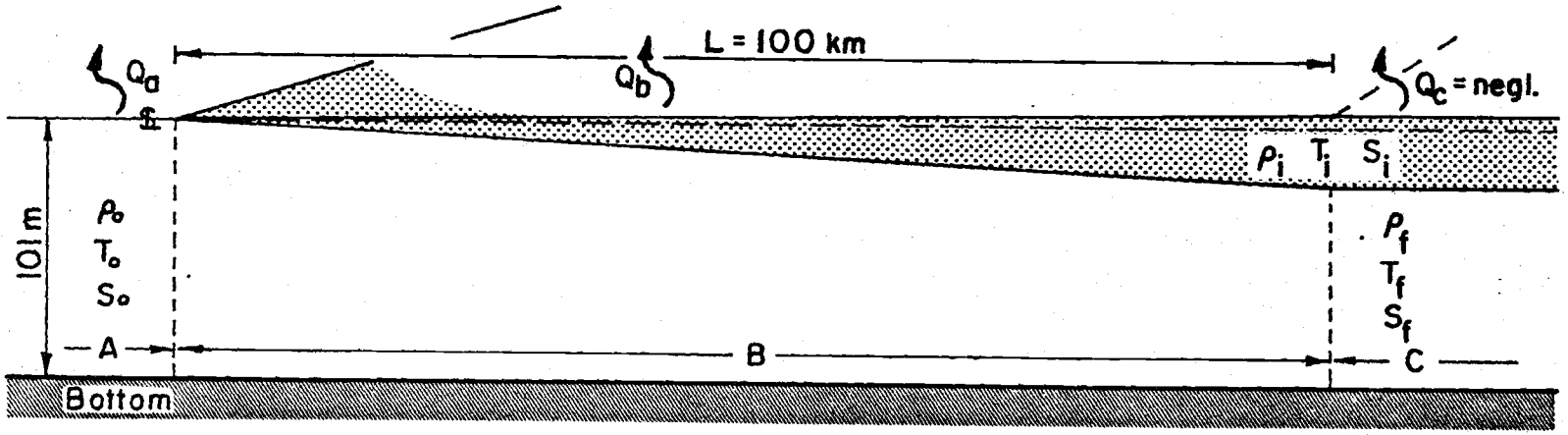


Fig. 2. Schematic model of a southward prograding ice front in a shallow marginal polar sea.

that the time from the commencement of salinity change to the onset of convection is

$$t_c = 27 \sqrt{\frac{\nu \rho}{g F_s}} \qquad (2)$$

where $\nu$ is the kinematic viscosity, $\rho$ is the density, g is gravity and $F_s$ is the salt flux. It is considered here that all of the water in the upper 1 m of sea water is converted to ice by the time that the trailing edge of the zone passes by and that the ice forming in the frontal zone is of uniform salinity $S_i$ = 5‰. (The 5‰ value is an average based on data given by Pounder (1962).) A total of three grams of salt per $cm^2$ of the 1 m-thick surface layer is excluded in $10^6$ sec, yielding a salt flux of $3 \times 10^{-6}$ gm $cm^{-2} sec^{-1}$. The corresponding time constant, from (2), is 70 seconds, a time much shorter than the 12 days of prograding time of the active freezing zone. As pointed out by Foster (1968) the underlying fluid into which haline convection begins is at that time essentially isothermal and isohaline, and it may be that the resulting salt fingers descend at terminal velocity since only weak dissipative forces will tend to stop the motion. Foster estimated velocities of the order of $10^{-1}$ to 1 cm $sec^{-1}$. For a 100 m water column the vertical transit time is then of the order of $10^5$ to $10^4$ seconds, which is small relative to the $10^6$ second progradation time of the freezing zone. Hence the

assumption that the excluded brine is rapidly distributed within the underlying fluid is justified.

From the salt flux computed above it is then inferred that the salinity of the fluid underlying the freezing zone increases to a maximum of $S_f = 35.30‰$ at the trailing edge of the zone. The corresponding freezing point depression is $T_f = -1.85\ °C$ and the density is $\rho_f = 1.0284435$. (Fig. 2)

Zone C. This zone is assumed to be quiescent insofar as further freezing is concerned. Hence the temperature and density of the underlying fluid are taken to be the same as the maximum values calculated for the trailing edge of zone B.

## B. The resulting pressure field.

The next step is to compute the depth of the one decibar pressure surface relative to sea level. In zone C, at a depth of 1 m the weight per unit area of the overlying ice column will be taken equivalent to that of an equal weight layer of fluid of salinity 5‰ and temperature of -1.85 °C. (i.e. supercooled). The problem is approached by first computing $\overline{V}$, the partial equivalent volume of sea salt in sea water of temperature 0 °C and salinity 35.0‰. Duedall (1966), gave:

$$\overline{V}(S‰,\ T\ °C) = a_{00} + a_{01}T + a_{02}T^2 + (a_{10} + a_{11}T)S \pm \varepsilon \text{ ml/eq} \quad (3)$$

where $a_{00}$, ... are empirically derived coefficients of T and S. The expression holds for the range $30 \leq S \leq 40‰$ and $0 \leq T \leq 25$ °C. Then, it is found V(35.0‰, 0.0 °C) = 13.74 ml $eq^{-1}$. Using the formula of Lyman and Fleming (1940), seawater of 35‰ contains 0.60536 equivalents per kilogram of seawater. Thus the partial volume of the sea salt at 0 °C and 35‰ is 8.3 ml per kilogram of sea water. It is assumed that the number holds for sea water at -1.8 °C and 35‰ within experimental error. Equation (3) is quasi-linear in S (i.e., $a_{11} << a_{10}$); thus the removal of 30‰ of salts from the freezing surface layer of original thickness of 1 meter removes also a volume which amounts to about 0.71 cm of vertical height. Thus the interface between the ice and the sublayer of enhanced salinity (35.30‰) will then be at 99.3 cm below sea level. It remains to determine the weight of the overlying ice column. This is estimated to be equivalent to that of a 99.3 cm column of fluid of 5‰ and supercooled to -1.85 °C. From sigma-t tables one obtains the density of the equivalent fluid as 1.0038490. The depth of the one decibar surface below the ice-water interface may then be computed as:

$$g[99.3 \times 1.0038490 + \Delta z \times 1.0284435] =$$

$$10^5 \text{ dynes cm}^{-2}, \text{ or } \Delta z = 2.4 \text{ cm.} \qquad (4)$$

The value of g is taken to be 983.53 cm $sec^{-2}$ for latitude 60 °N (Neumann and Pierson, 1966). Thus, in zone C, the depth of the one decibar pressure surface below sea level is 99.3 + 2.4 = 101.7 cm. In zone A, the depth of the one decibar surface is computed from

$$gz_A \times 1.0281994 = 10^5 \tag{5}$$

by which $z_A$ = 99.0 cm.

C. Relative current and transport under the freezing zone.

The slope of the one decibar surface is now computed as

$$i = \frac{101.7 - 99.0}{(L = 10^5)} = 2.7 \times 10^{-7} \tag{6}$$

and a corresponding geostrophic current of $v_g = igf^{-1} \doteq 2.2$ cm $sec^{-1}$, directed to the east.

The justification for assuming geostrophic balance is made by examining the Rossby number, R = U/fL, which may be interpreted as a ratio of acceleration to Coriolis forces. For a velocity amplitude U = 2 cm $sec^{-1}$, a characteristic length scale L = $10^7$ cm, and f of the order of $10^{-4}$, the Rossby number of $10^{-3}$ shows that the time scale of geostrophic adjustment, 1/f, is relatively small compared to that of the basic flow field, U/L; hence the geostrophic

assumption is justified.

The baroclinic field in a north-south section is shown in Fig. 3. Since it has been assumed that the ice pack once formed develops no leads, the bottom is both isobaric and level. For a baroclinic field linearly decreasing with depth the vertically averaged geostrophic velocity $v_g$ of the water column is 1.1 cm $sec^{-1}$ over the entire 100 km wide freezing zone. The resultant volume transport is computed as the product $v_g \cdot D \cdot \Delta y$, yielding a value of $10^5$ $m^3$ $sec^{-1}$, or 0.1 Sverdrup.

D. Transport as a function of the geometry of the system.

Transport is invariant to the width of the freezing zone, L. For example, doubling the active zone width to 200 km halves the slope of the pressure surfaces and, for the same water depth, yields the same volume transport.

However, an increase in the depth to which the excluded brine is convectively mixed does increase the transport, other factors remaining the same. It can be shown that the transport is proportional to the decrease in total potential energy of the ice-water column which results from the downward distribution of excluded salts.

Consider the model in Fig. 4 in which a surface layer of sea water of height h is to be frozen. The fluid is taken initially to be homogeneous in density, i.e. $\rho_2 = \rho_1$. The initial total potential

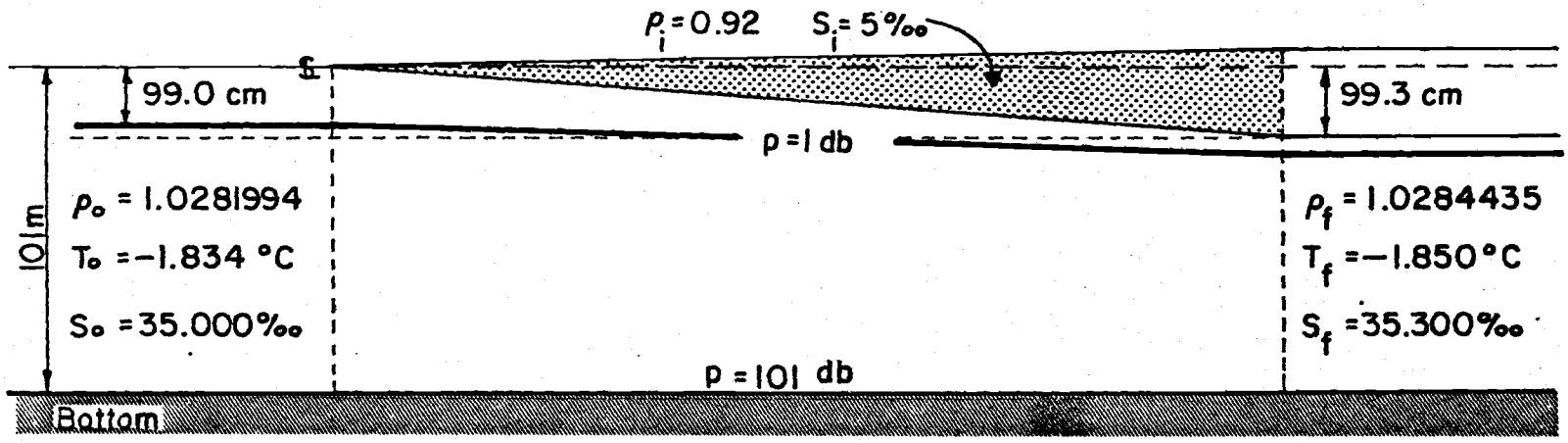


Fig. 3. A vertically-magnified diagram of the slope of the 1 db pressure surface in the shallow marginal polar sea model.

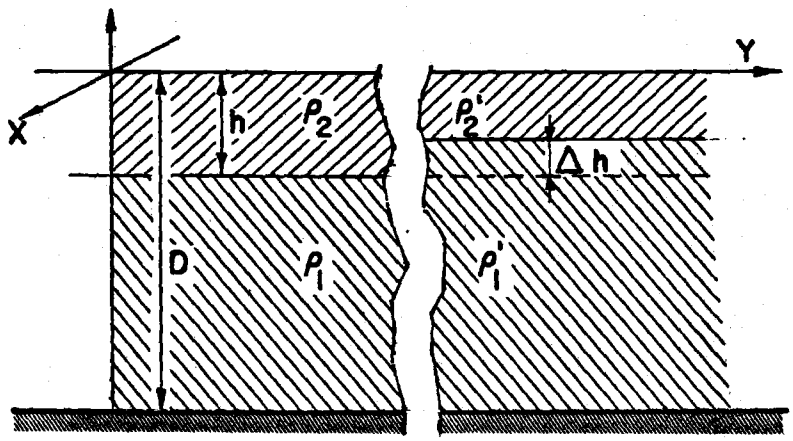


Fig. 4. Schematic model of an initially well mixed, shallow ocean in which a surface layer, h, is to be frozen.

energy of the water column is

$$PE = \underline{PE}_1 + \underline{PE}_2 = - \frac{\rho_1 g D^2}{2} . \qquad (7)$$

Now we introduce a membrane at level h and transfer salt from layer 2 downwards into layer 1, allowing h to shrink by an amount $\Delta h$ to account for the loss of the partial equivalent volume of salt in layer 2. The total potential energy of the new system after salinity of layer 2 is decreased by a factor $\Delta S_2$ is

$$PE' = (h - \Delta h)^2 \cdot \frac{g}{2} \cdot (\rho'_1 - \rho'_2) - \frac{\rho'_1 g D^2}{2} \qquad (8)$$

The change in total potential energy, $PE = PE - PE'$, is given by

$$\Delta PE = \frac{g}{2} [ D^2 (\rho'_1 - \rho_1) + (h - \Delta h)^2 (\rho'_1 - \rho'_2)] \qquad (9)$$

The densities of the layers are of course related through the equations of state

$$\rho_1 = \rho_2 = \rho_0(1 - \alpha T + \beta S);$$

$$\rho_1 = \rho_0[1 - \alpha T + \beta (S + \Delta S_1)]; \text{ and}$$

$$\rho_2 = \rho_0[1 - \alpha T + \beta (S + \Delta S_2)] \qquad (10)$$

where $\Delta S_1$, $\Delta S_2$ are the changes in salinities due to the transfer of salt across the membrane and are related by $\Delta S_1 = -(h/D)\Delta S_2$, and $\alpha, \beta$ are the thermal expansion and saline contraction coefficients, respectively. In this problem, the term $\alpha T$ is negligible insofar as changes in density are concerned. Substituting eq. (10) into (9) and noting that $\Delta h : h : D$ as $1 : 10^2 : 10^4$, the total change in potential energy of the water column is thus approximately

$$\Delta PE \simeq -\frac{\rho_0 g}{2} (\beta \Delta S_2) Dh \qquad (11)$$

The phase change, water to ice, of the surface layer $(h - \Delta h)$ creates a positive $\Delta PE = gh^2(\rho_{water} - 1.21\ \rho_{ice})$; however, this term is at least two orders of magnitude smaller than the terms in equation (11) and is therefore negligible.

Equation (11) states that the decrease in potential energy of the water column is directly proportional to the depth D to which convective mixing occurs, and to the thickness and salinity change of the

surface layer to be frozen.

Equation (11) can also be written as

$$\Delta PE = -\frac{g}{2}(\rho'_2 - \rho_2) \cdot D \cdot h \qquad (12)$$

and the expression for the eastward volume transport can be written as

$$T_x = \overline{V}_g \cdot D \cdot \Delta Y = \tfrac{1}{2} i_s g f^{-1} \cdot D \cdot \Delta Y \qquad (13)$$

where $i_s$ is the slope of the one decibar surface and $\Delta Y$ is the width of the active freezing zone. Solving for D in both expressions (12) and (13) and equating, we have, after some manipulations,

$$T_x = -\frac{1}{\rho f} \cdot \Delta PE \cdot \left[ \frac{\Delta P_h}{gh(\rho'_2 - \rho_2)} \right] \qquad (14)$$

where $\Delta P_h$ is the pressure change at level h following the transfer of salt. The bracketed term is dimensionless and of order unity. Thus it is possible to write

$$\rho T_x = -\frac{1}{f} \Delta PE \qquad (15)$$

which states that the eastward mass transport is proportional to the decrease in the potential energy of the water column. The constant of proportionality is the inverse of the Coriolis parameter.

## E. Limitations of the basic model.

The model developed in these past sections is constrained by the initial conditions and assumptions imposed at the beginning of its development. Most assumptions remain valid in an application of this model to a real shallow, marginal arctic sea, (i.e. the Bering Sea shelf), with the exception of the fact that an initially motionless ocean has been considered. Little is known about the circulation of marginal polar seas during freeze-up conditions. However, existing evidence suggests that some sort of circulation exists over the shelf of these polar seas just prior to the formation of ice. Therefore an interaction must exist between that circulation and the baroclinic flow explained in this chapter. This possibility is explored in the following sections.

# III. THE ADVECTION MODEL: RECTILINEAR MOTION

It is now assumed that there is established circulation prior to the beginning of ice formation and a model that examines the consequences of such an advection is developed based on the model introduced in the preceding section. This model will consider only an initially homogeneous rectilinear motion of the fluid, at the onset of freezing.

Fig. 1 also illustrates the new situation. Let $\underline{U}$ be the advection vector referred to the same coordinate system employed in the last section, and therefore having components $U_1$, $U_2$ and $U_3$. $U_1$ is the component in the east-west direction and therefore in the direction of the circulation induced by the progradation of the ice front, as was shown in the development of the basic model. If this component exists, it will add algebraically to the induced circulation, without much other effect, the model being considered infinite in the X direction. The component $U_2$ is in the north-south direction and therefore in the direction of advance of the ice front. It is thus expected to have some effect on the density distribution and hence on the east-west induced circulation and transport. The $U_3$ component, which is the vertical component of advection, will be considered negligible insofar as its interaction with the downward mixing of salts is concerned. Therefore, the only component left to consideration is the $U_2$ component

which will be shown to play an important role in the distribution of mass in the model situation.

## A. Description of the model.

The fluid will be considered incompressible and all changes of density will be attributed to the salt flux and to the advection of mass due to the $U_2$ component. That is, no consideration is made of the effect of temperature variations on the density distribution for the same reasons expressed in the preceding section.

It is necessary to define a velocity of the fluid (advection) relative to the advancing ice front. Let the velocity of progradation of the ice front be denoted by $\underline{C}$, equal to 10 cm $sec^{-1}$ directed to the south. Then the north-south velocity of the fluid relative to that of the ice front will be denoted by the quantity $(C-U_2)$. It is then clear that in this situation the amount of salt received by a given water column is dependent on the velocity of the water, all other factors remaining the same. The time during which salt will enter a given unit column of water is thus $t = L/(C-U)$, where the subscript has been omitted for U since it is the only component considered. Then the amount of salt absorbed by the underlying fluid is given by

$$\Delta S = F_s \left[ \frac{L}{(C-U)} \right] \quad \text{gm cm}^{-2} \tag{16}$$

which is the expression for the time dependent salt input to the

subjacent water. The corresponding change of salinity is given by:

$$\Delta S = \frac{F_s}{D} \cdot \frac{L}{(C-U)} = \frac{3 \times 10^{-3}}{(C-U)} \quad \text{gm cm}^{-3} \qquad (17)$$

B. Three possibilities.

It is possible to introduce at this point three main cases in the model, depending on whether the relative velocity of the underlying fluid (C-U) is equal, less, or greater than zero. The three cases are examined in this section.

Case A, [(C-U) = 0].

This special case, where the relative velocity of the water and the ice front is zero, implies that it is possible to find the same parcel of water under a given point of the ice front during the evolution of the process. Figure 5 illustrates this case, where the model is depicted at two different times and the shadowed area indicates the water of enhanced salinity. Thus care should be taken when considering this case, since the expression (16), derived for a time dependent salt input goes to infinity. Rather, the time factor in equation (16) that indicates the time during which the salt is entering a given unit column of water should be simply replaced by the time the ice front has been advancing. It has been stated during the development of the basic model that the time that the process lasts is of the

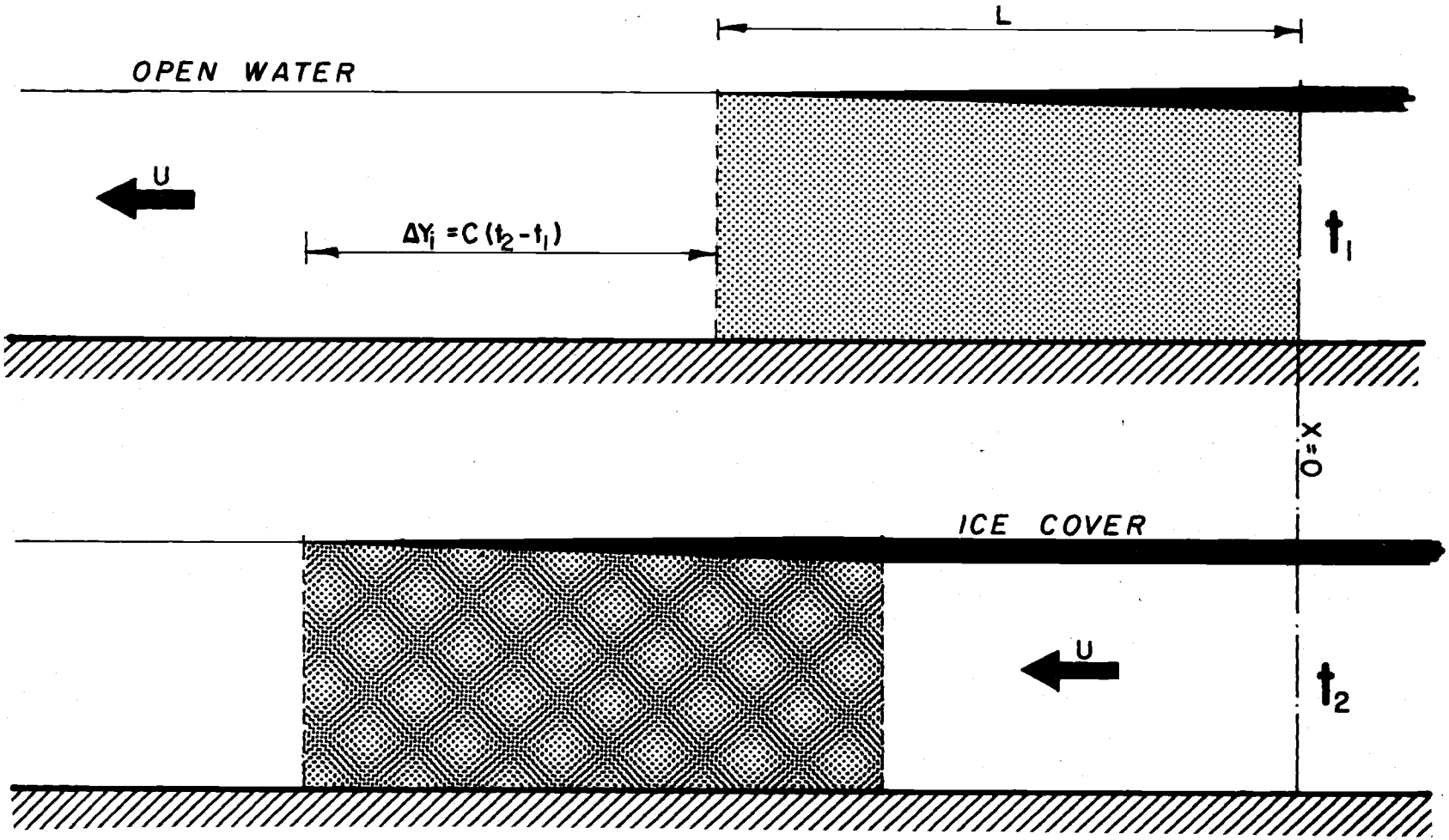


Fig. 5. Evolution of the system for the case [(C-U) = 0]. [Case A].

order of three months, or approximately $10^7$ sec. Therefore, the maximum amount of salt that may be absorbed by a given water column is of the order of $(3 \times 10^{-6})(10^7) = 30$ gms $cm^{-2}$ of salt. Since it has been assumed that the process occurs in 100 m of water, the corresponding change of salinity is 3.0‰, a considerable one.

Thus, if the motion of the water constantly followed the ice front advance, it should be possible to find water of salinity 38.0‰ under the ice front at the end of the freezing season. The resulting density distribution will be such as to have a region of lower density south of the front, which is constituted by the original water of salinity 35.0‰, followed by the very high density water under the ice front. By original water it is meant the water of regional characteristic at the beginning of the freezing season. A sharp horizontal density gradient is thus formed at the leading edge of the front. (Fig. 5). To the north of the ice front, it will be possible to find water that will be assumed not to have received salt from the sea-ice formation. This implies the presence of another density gradient at the trailing edge of the front, but of opposite sign than the one under the leading edge.

The resultant distribution of pressure is such that the system tends to form a circulation pattern consisting of two jets with opposite flow directions, one under each edge of the front. Following the basic model, the jet under the leading edge of the front will be an eastward

flow. The trailing edge jet is thus expected to be flowing to the west. This situation is depicted in Fig. 8a.

Case B. [(C-U)< 0].

In this case the velocity of the fluid is less than or opposite in direction to the advance of the ice front. The water "lags" behind the ice front in its southerly progradation and fluid of enhanced salinity is found under the ice cover north of the trailing edge. The evolution of this case is shown in Fig. 6.

Obviously, the case of an initially motionless ocean discussed in the development of the basic model is a particular example of this case where (C-U) = C or U = 0. (Fig. 2).

The salt input into the water in this case is given by

$$S = \frac{F_s}{D} \cdot \frac{L}{C} = \frac{3 \times 10^{-3}}{10} = 3 \times 10^{-2} \text{ gm cm}^{-3} \qquad (18)$$

which corresponds to a salinity change of 0.3‰, the value obtained previously. The resulting eastward circulation and transport have been amply discussed in chapter II, and illustrated in Figs. 2 and 3. A sketch of the circulation pattern for case B in general is depicted in Fig. 8b.

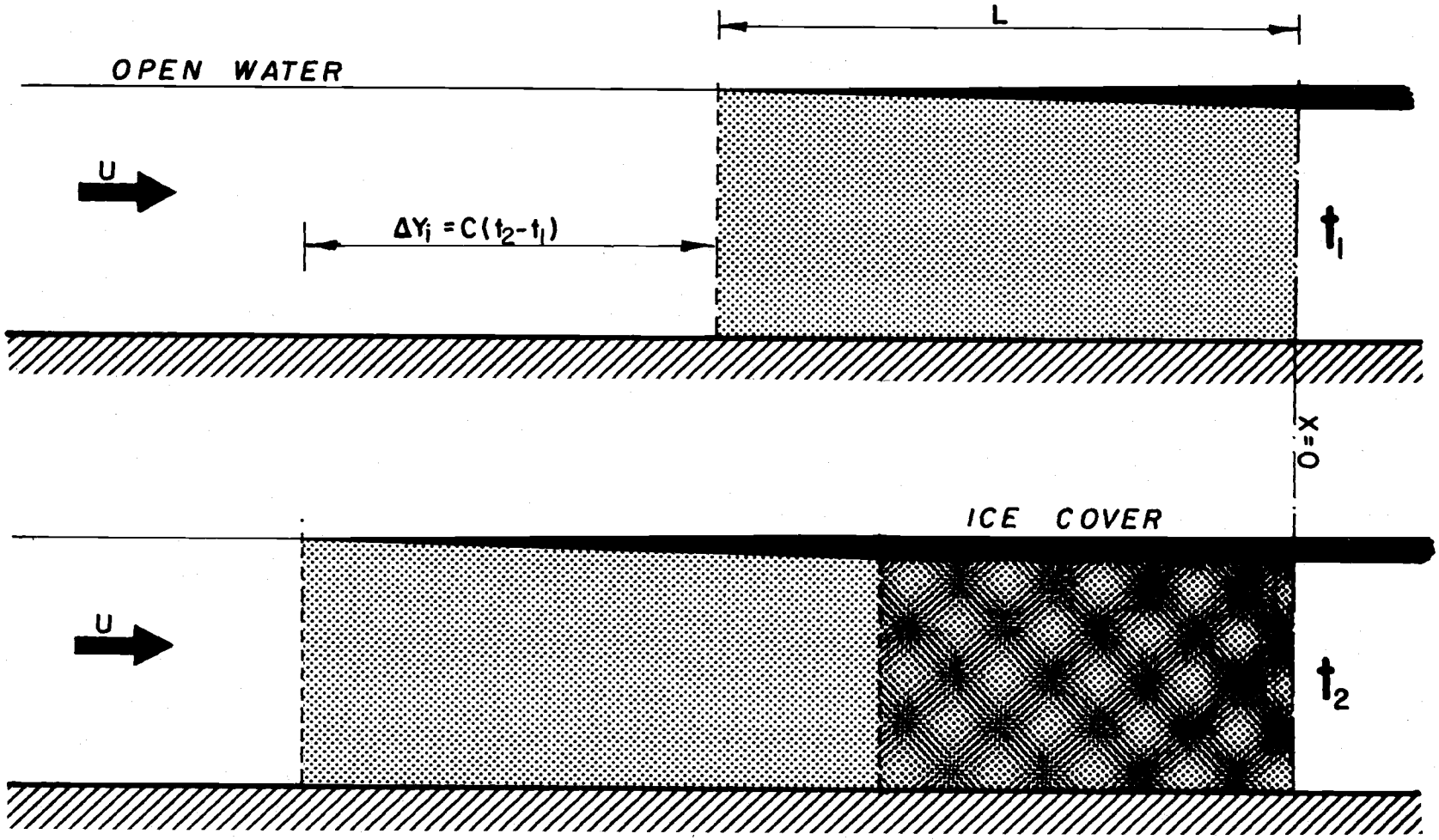


Fig. 6. Evolution of the system for the case [(C-U) < 0]. [Case B].

Case C. [(C-U) > 0].

Finally it is possible to encounter the case where the velocity of the water is in the same direction as the ice front progradation but of a greater magnitude than C. The evolution of case C is depicted in Fig. 7. It can be seen that the fluid moves in a southward direction at a faster speed than the ice front, advecting water of enhanced salinity past the leading edge of the front into open water. Therefore, the density distribution will be such that the original water of salinity 35.0‰ will be found well to the south, separated from the front area by the fluid of enhanced salinity that has been advected past the front. These two waters thus form a horizontal density gradient well to the south of the front, in open water. North of the trailing edge of the front, under the ice cover, lies water that has not received salt from the sea ice formation and is therefore of lower salinity than the water under the front. Therefore, it is possible to find a second horizontal density gradient under the front, due to the salt flux from the forming ice. Of course, the position of the first density gradient will depend on the value of (C-U).

The corresponding flow regime is shown in Fig. 8c. Following the basic model, the first density gradient mentioned above will cause an eastward flow, shown in a left hatching, while the density gradient under the front will cause a return flow to the west (right

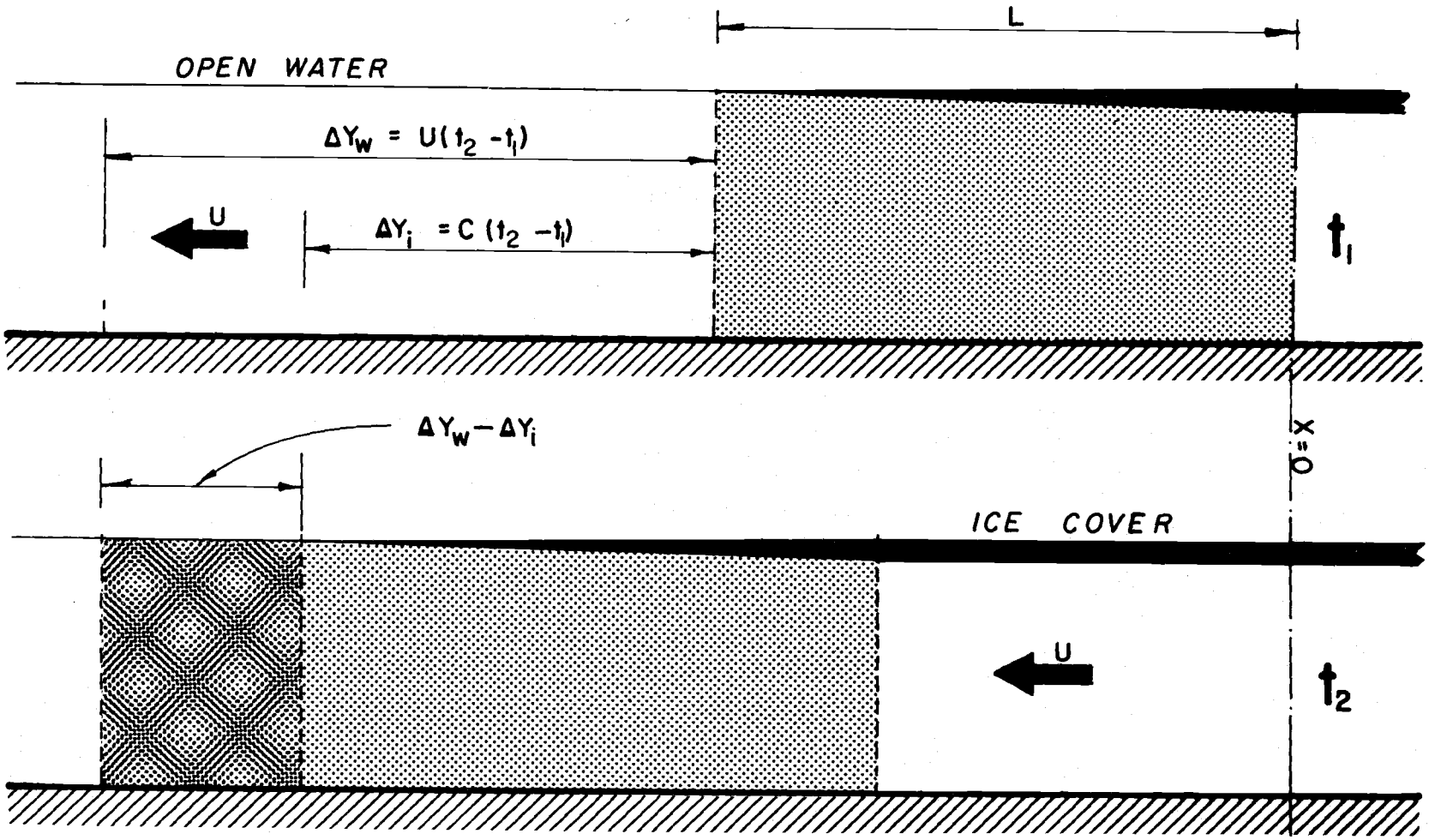


Fig. 7. Evolution of the system for the case [ (C-U) > 0]. [Case C].

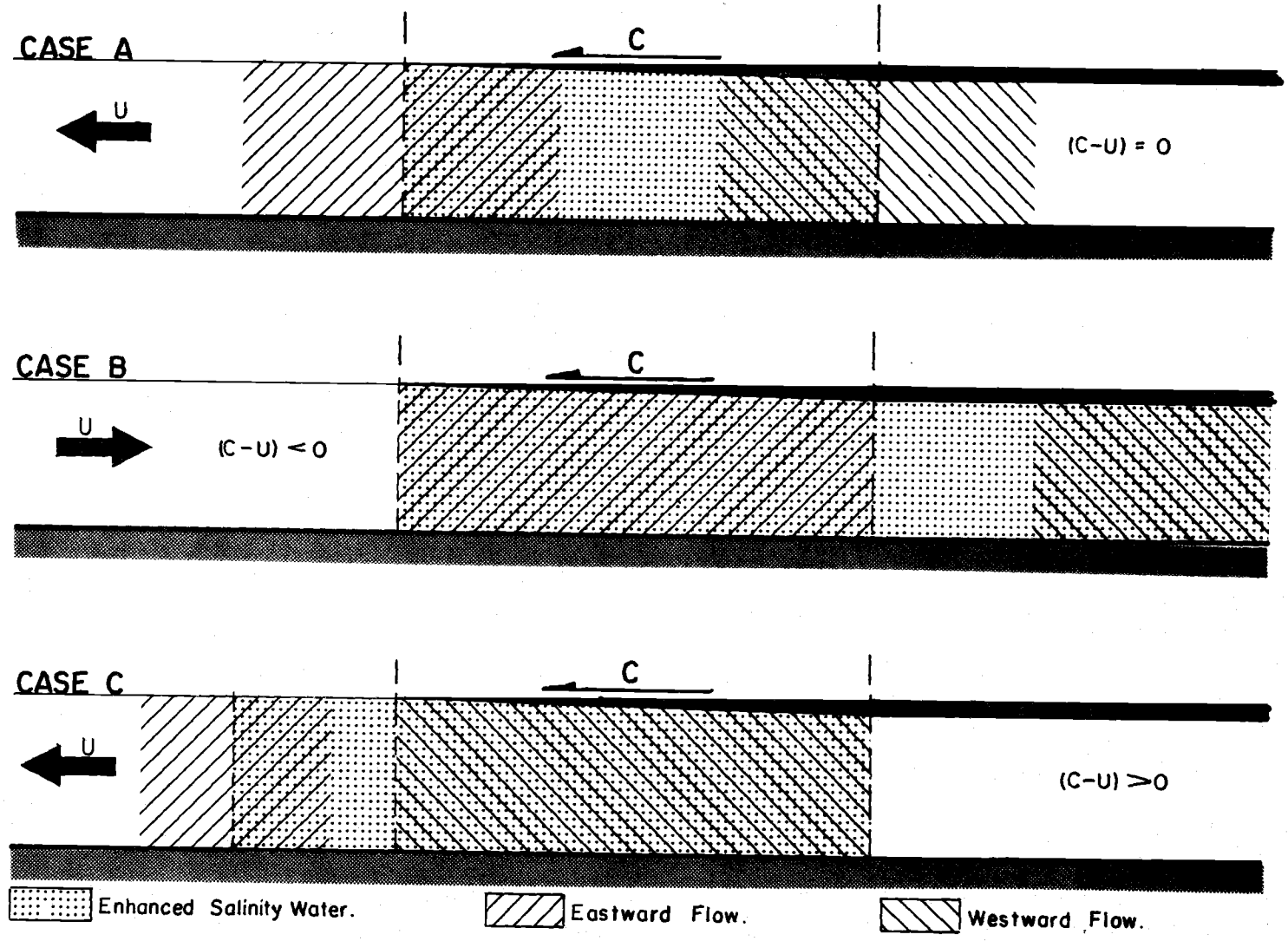


Fig. 8. The flow regime for the three cases.

hatching).

Figure 8 illustrates the ensemble of the circulation patterns for the three cases examined in this chapter. As mentioned above, the shading indicates water of enhanced salinity, that is, that has been subjected to the salt input from the formation of sea ice and the hatching indicates the different directions of the flows. It is observable that each case induces a circulation in the region of forcing, the ice front, and that for the two cases where the velocity of the fluid is different from the speed of the ice front progradation, a compensating flow is found, which is removed from the region of forcing. For case B, the induced circulation is an eastward flow and the compensating flow takes place in the form of a westward flow to the north of the ice front, under the ice cover. For case C, the induced circulation is a westward flow under the front, and the compensating flow takes place as an eastward current south of the ice front, in open water. The transition point between the two cases is what has been described as case A, where both flows are found under the edges of the front. This general situation will be an important one in the next chapter, where the interaction of the ice formation with a circular motion is examined.

# IV. CIRCULAR MOTION

The models developed in the preceding sections permit considerable insight about the effects of sea ice formation processes and their interaction with a pre-established circulation. The advection-interaction model of chapter III considered only that a homogeneous rectilinear motion of the fluid was allowed to exist. However, a typical ocean contains gyres and eddies. The causes for such circulatory motions are very diverse and therefore the eddies can show great variations in their typical scale. Thus it is considered necessary here to analyse the possible effects of the interaction of the ice front with circular motions, and an idealized case will be considered in this section, which is illustrated in Fig. 9.

Suppose the ice front encounters in its progradation a circular motion of the fluid in the form of a gyre whose center will here be considered fixed. It will be assumed that the tangential velocity $\underline{V}$ in the external part of the gyre is greater than the speed C at which the ice front progrades. The radius of the gyre will be assumed for further convenience to be of the order of the chosen length scale L, or less. Suppose furthermore that the sense of rotation of the gyre is clockwise, solely for the purpose of this discussion.

In order to conduct the analysis of this section, it will be apparent that the motion of the gyre may be firstly decomposed into

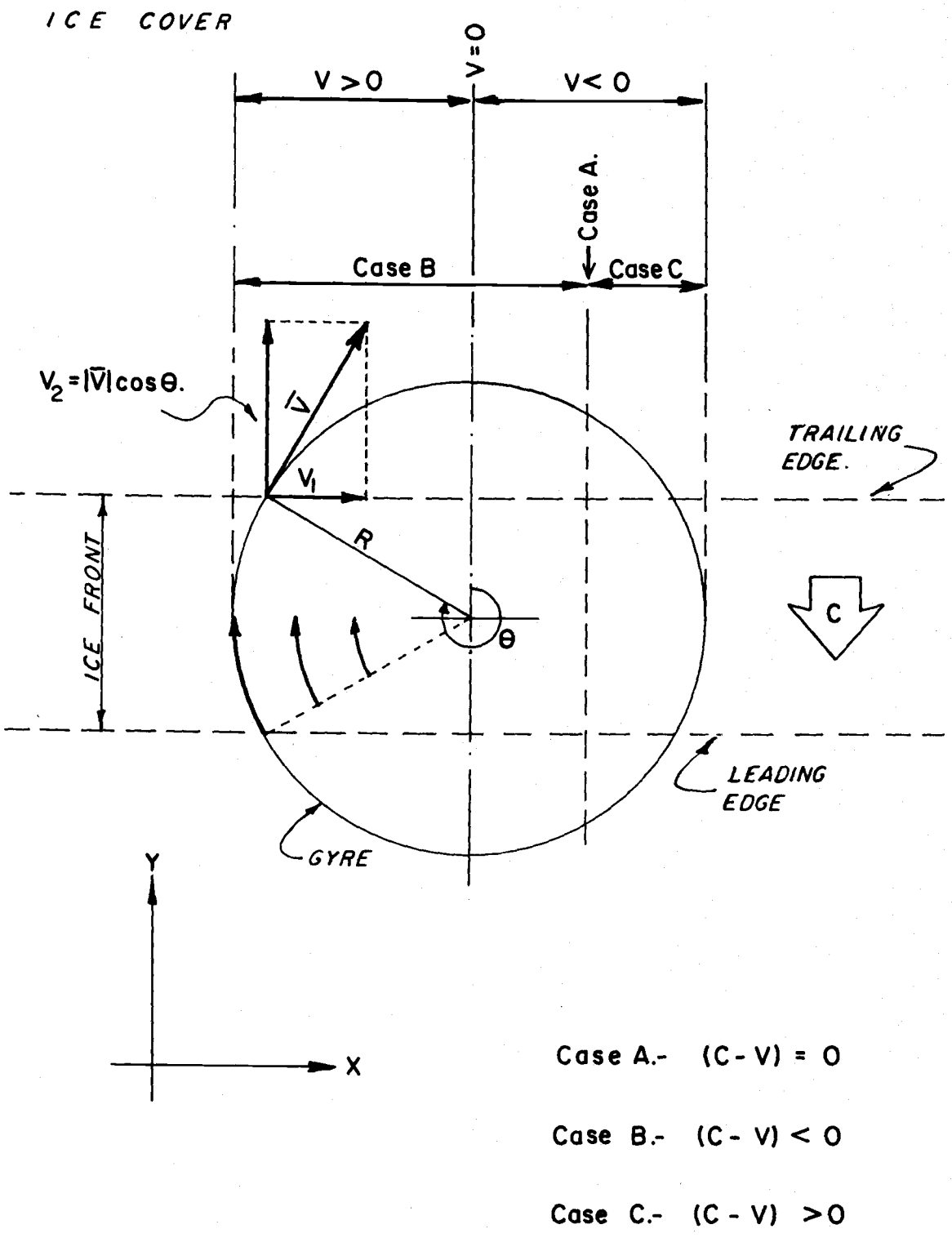


Fig. 9. Interaction of the ice front with a gyre.

its components. The velocity $\underline{V}$ has components $V_1$ and $V_2$ where, in analogy with the advection $\underline{U}$ in the preceding section, $V_2$ is in the north-south direction and will be the only one considered. Therefore, the subscript will henceforth be dropped. The velocity V is given by

$$V = \overline{V} \cos \theta \tag{19}$$

and it is apparent (Fig. 9) that it is possible to distinguish regions within the gyre in which the velocity V is positive, negative or equal to zero. This brings forth the possibility to consider now a relative velocity of the fluid with respect to the ice front progradation speed, C. It is clear from the development of the preceding section, that the relative velocity will be expressed as (C-V) and furthermore, that it is possible to distinguish separate regions within the gyre where the relative velocity is positive, negative, or equal to zero. In other words, it is possible to decompose the gyre motion into the three cases exposed in the model of chapter III. (Fig. 9). Firstly, it has been shown that the velocity V is equal to zero in the north-south center line, denoted by (V = 0) in Fig. 9. This will then correspond to the situation depicted in the development of the basic model. (Figs. 2, 6 and 8b). To the east of this line, the V component is increasingly negative until it reaches a value equal to C, the speed of the ice front. At this point, the two velocities are equal and (C-V)

being equal to zero, case A (Chapt. III), applies. To the east of this region, the velocity of the fluid is greater than that of the ice, thus advecting water of enhanced salinity towards open water and, as shown in Fig. 9, case C applies. (Figs. 7 and 8c). To the west of the C = V line, case B is predominant (Figs. 6 and 8b), and the fluid velocity is such that salt will be advected to the north of the ice front, under the ice cover.

Correspondingly, a density distribution, pictured in Fig. 10, can be inferred for this situation from the density distribution of the three cases of chapter III. Figure 10 indicates the three regions that correspond to said cases with reference to the cross sections illustrated in Fig. 8. The shading indicates water of enhanced salinity and the heavier shading indicates water of the highest salinity, that is, water that has been advected completely under the ice front. To the west of the (C-V) = 0 line, the water is "lagging" in the southward motion with respect to the ice front, whereas to the east of the same line, the water has been displaced past the front and higher salinity water is found south of the front. It is clear, therefore, that the interaction of the ice front with the gyre presents the three possibilities discussed previously, and that Fig. 8 is suitable as a vertical representation of the process in a north-south section.

Furthermore, in chapter III, the resulting flow regime for each of the cases has been discussed, noting that all of them presented a

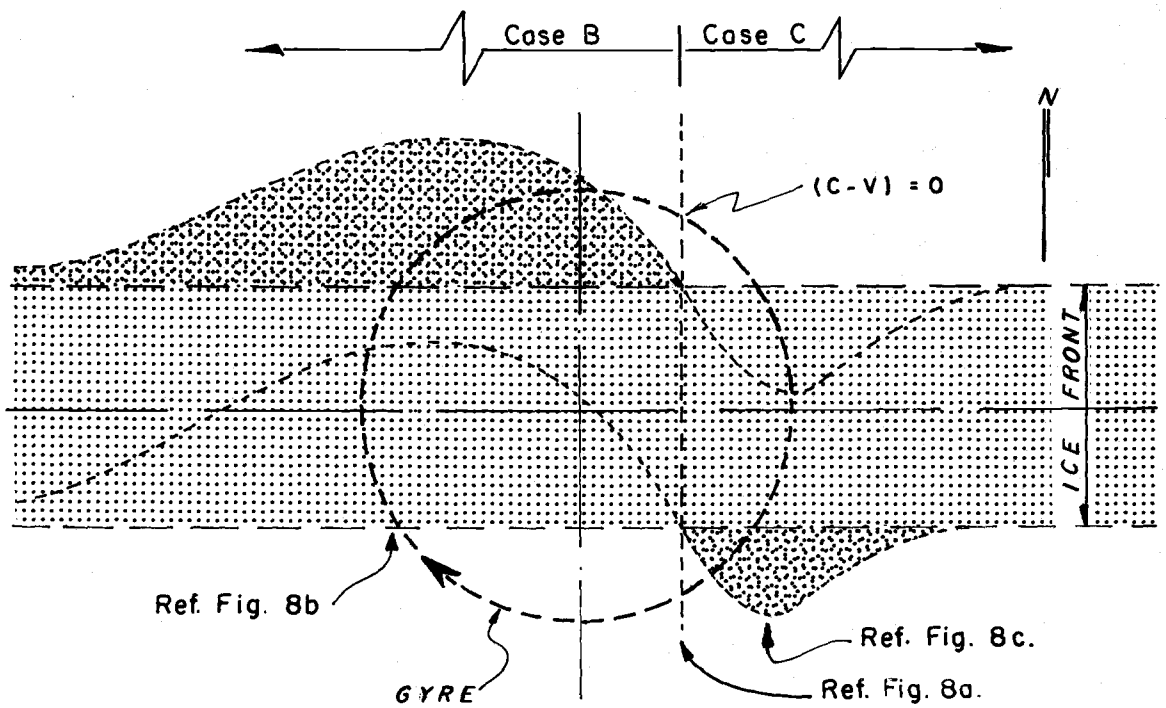


Fig. 10. Density distribution resulting from the interaction of the ice front with a gyre. [Note the three cases of relative velocity.]

main flow under the ice front and a compensating flow removed from the region of forcing, exception made of case A, where the two flows occur under the front with what could be expected as a reasonably equal intensity. Figure 11 depicts the flow regime resulting from the interaction of the ice front with the gyre. It can be noted that on each side of the (C-V) = 0 line there exists a main flow under the ice front and a compensating flow which is here depicted in the form of a jet. The (C-V) = 0 line acts as a transition region where each main flow becomes the compensation jet of the opposite main flow. The result is that in that region, both flows are equivalent in intensity and width, in accordance with the scheme of case A and Fig. 8a.

Therefore it is seen that the resulting flow regime is one that tends to counteract the gyre to some extent. A distortion of the circular motion of the gyre must occur and it is here speculated that the end result may be the destruction of the gyre by the effect of the ice front salt input. It is also speculated that some appreciable speeds must be generated by the process, perhaps in the order of one magnitude greater than that obtained in the development of the basic model in chapter II. However the time dependence of the process is clear and a precise answer to these speculations can be obtained only through another type of modeling, e.g. numerical modeling.

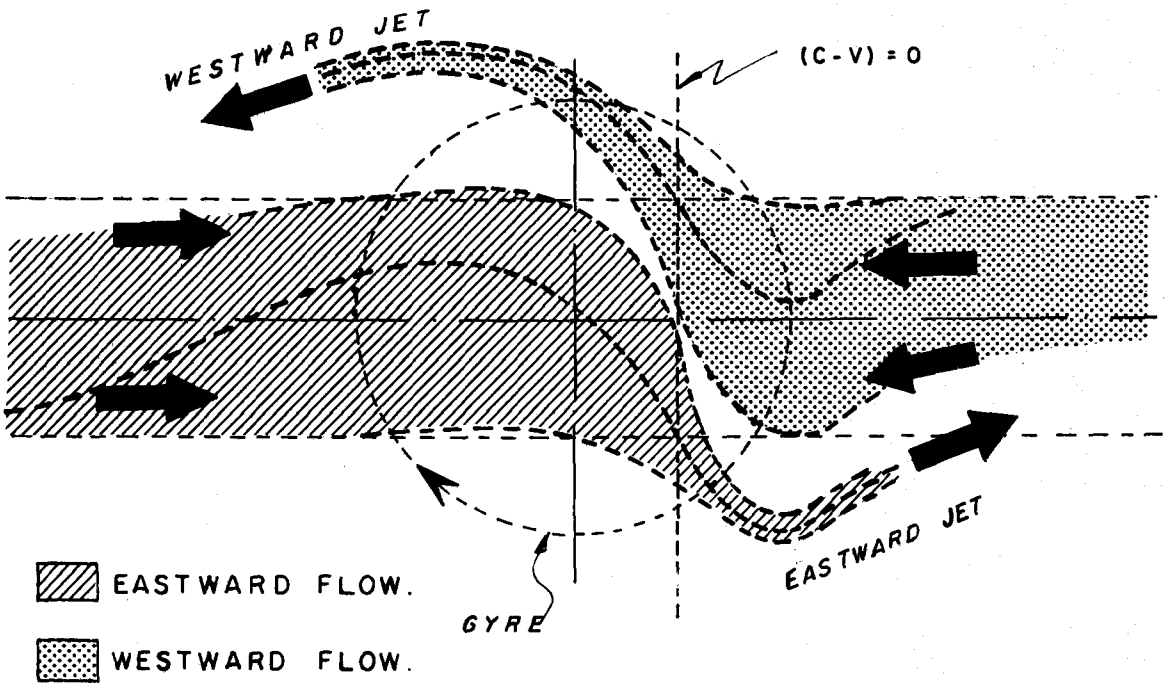


Fig. 11. The resulting flow regime.

# V. DISCUSSION

It has been shown that an advancing ice front which is an idealization of the usual way a marginal polar sea freezes, induces a change in the potential energy of the water column through a downward mixing of the excluded salts. The resulting baroclinic circulation extends to the depth of penetrative convection which has been taken to be the bottom for purposes of this model. The flow is otherwise bounded by the trailing and leading edges of the front and may be directed to the east or to the west if the advection of the underlying fluid is to the north or to the south, respectively, relative to the ice front.

This has been arrived at by means of arguments based on assumptions that may be shown to be reasonable. The assumption that the freezing zone extends over 1° of latitude, or about 100 km is not only a convenient scale, but corresponds roughly to the scale at which relevant mesoscale atmospheric temperature gradients occur. Furthermore, it has been demonstrated above that the transport is independent of the width of this zone, thus eliminating any inaccurate results related to transport. The assumption of a linear northerly increase of the ice thickness within the freezing zone is probably not an accurate one but neither is it critical. The assumption that the bottom is both an isobaric and a level surface may not hold in the

event that the ice develops leads, since the fluid in the leads is of higher salinity than the original surface water. However, Solomon (1969) has studied this case and shown that a barotropic component of the flow may be induced in a direction perpendicular to the ice front, but its magnitude is small. Furthermore the system of leads can be thought of as a mesoscale phenomenon of the same scale as the meteorological phenomena mentioned above, and thus having only an overall effect on a considered region, but not affecting processes of the length scale considered here.

It has been further assumed that the thickness of the ice at the trailing edge is of the order of one meter. This is certainly a good order-of-magnitude approximation and therefore constitutes a convenient assumption. The assumption that the freezing rate behind the active zone is negligible is probably close to reality, considering the insulating properties of the sea ice and the related snow cover. Considering the shelf as having a uniform depth of 101 m is a simplifying assumption which allows for the freezing of the top meter of water, according to Fig. 4, and with 100 m of water remaining under the developed ice cover to absorb the excluded salts. This is also a good approximation within an order of magnitude, for a marginal Arctic Sea.

Thus the model seems reasonable. Under the assumptions stated above and in the frame set in chapter II, the model yields an

eastward transport of 0.1 Sv. Over a period of three months the total transported volume would be in the order of 1000 $km^3$. It has also been shown that current speeds of the order of 2 cm $sec^{-1}$ can be expected for the basic model. This figure may vary, since it is reasonable to expect that in case A, when the basic flow tends to become a confined jet (Figs. 5, 8a, 10 and 11), the velocities to be encountered may exceed said value largely. In the same way, in cases B and C, if the advection U is large, it may be possible to find values for the induced currents that are hardly significant.

These values compare favorably with generally accepted values reported for marginal Arctic Oceans which seem to range between an order of 1 to 10 cm $sec^{-1}$ (Hughes et al., 1974) although the high extreme of the range has been reported principally in straits. Reported values for transports in the same areas are of the order of 10 Sv which is considerable compared with the value here obtained. This of course rises from the fact that the scale of the process being analyzed is much less than the global phenomena reported in the literature. Therefore, the scheme presented here can be considered as being important mainly in regions where there exists an interaction of the front with circular motions as was exposed in chapter IV, since it was shown that the system has a tendency to form jets of higher speeds. It must be kept in mind also that the transport is perpendicular to the advance of the ice front. But most marginal

Arctic Seas are oriented in a north-south direction and therefore, the main circulation in them is also oriented in the same direction. Therefore, the transport induced by the ice front progradation may be of importance, since it acts in a direction whose components are generally small.

This importance should have a noticeable impact in the explanation of some physical and biological phenomena.

## A. Application to the Bering Sea Shelf

In this section an example is given of the application of the models developed in the previous chapters to a typical marginal shallow Arctic Sea: the shelf of the Bering Sea.

The continental shelf of the Bering Sea is roughly rectangular in shape, extending over 1000 km northwest to southeast and some 500 km northeast to southwest, from the Bering Straits at 66 °N to Bristol Bay at approximately 58 °N. Most of the continental shelf waters in the eastern Bering Sea are shallower than 100 m (Takenouti and Ohtani, 1974). (Fig. 12). In late summer it is clear of ice and by mid-winter the ice pack is advanced to a position roughly coincident with the southern edge of the shelf. Thus the ice advance is approximately 700 km which is a good approximation to the assumption made in chapter II. Since the freeze-up of the Bering Sea occurs in about three months, the concept of a prograding speed for the ice

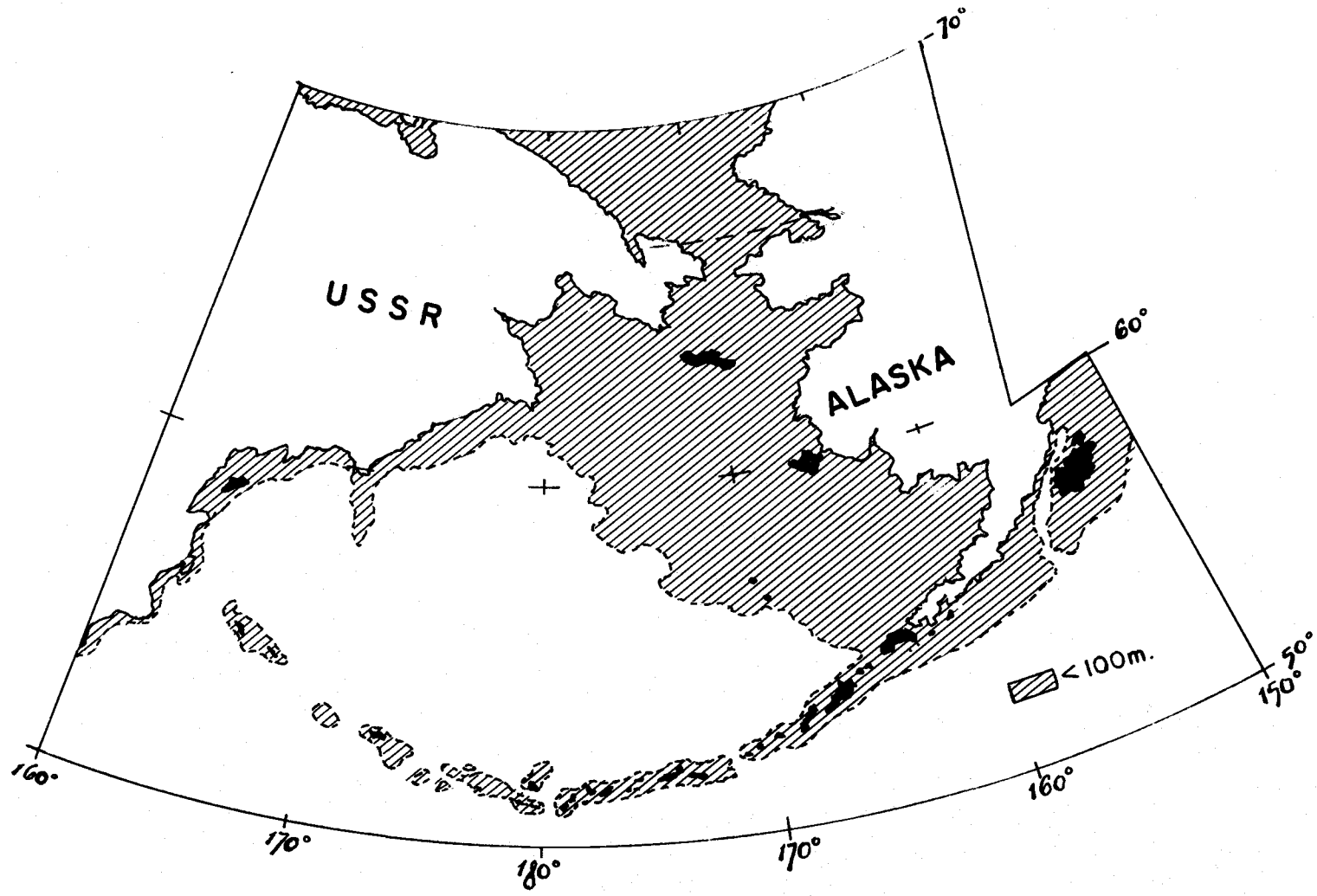


Fig. 12. The Bering Sea shelf.

front of 10 cm $sec^{-1}$ remains valid. In this case also, the assumption of a well mixed water column is considered valid. Although very little is known about the hydrography of the Bering Sea shelf during freeze-up, the USCG Icebreaker NORTHWIND took three stations in the region around St. Lawrence Island, from 63° to 64 °N and from 170° to 172 °W, in February 1969. Two of the three showed nearly isothermal, isohaline conditions, with a maximum of 0.05 sigma-t units density difference from surface to bottom (58 m) (Neshyba, pers. comm.). Russian investigations were summarized by Gershanovitch et al. (1974): "In the shallow areas of the Bering Sea, local distribution of water masses occurs in summer. In winter the waters of the shallow areas are isothermal. As the ice edge is approached, the temperature drops to below zero."

Thus it is clear that the models developed here are valid for portions of the Bering Sea, particularly the shelf area. It has been mentioned that the model yields a transport of 0.1 Sv. Over a three month freeze-up the total fluid transported through a given meridional section is of the order of 800 $km^3$, which is about 10% of the total volume of the shelf region assuming an average depth of 100 m. Clearly, the effect on winter circulation would be significant, for the shelf of the Bering Sea.

However, the Bering Sea shelf does not allow the assumption of an initially motionless ocean to be valid. Indeed, a pre-established

circulation exists, which is poorly known, especially just prior to the freeze-up season or during the advance of the ice front. Most methods of determination of currents employed in that area have been of the indirect type and no precise scheme for the flow regime has been established. However, some authors have presented what is considered the general current pattern for the Bering Sea (Arsen'ev, 1967; Favorite, 1974; Takenouti and Ohtani, 1974; Hughes, 1974; Cameron, 1974). Figure 13 is taken from Arsen'ev (1967), and seems to summarize satisfactorily the accepted views on the Bering Sea circulation. The outstanding observable features are the gyres over the shelf and a broad flow to the north, close to the American continent. A smaller flow to the south is observable close to the Asian continent. This suggests that during the season of ice formation, the three cases of chapter III and the interaction model of chapter IV apply. A quantitative result is difficult to obtain due to the time dependence already explained, but a qualitative description of the ice front with the existing circulation following Arsen'ev's scheme is proposed in Fig. 14. The figure illustrates the process at a given point in time, and it can be seen that the presence of the gyres may promote some circulation patterns with appreciable speeds. It is very probable that these patterns be detectable in field experiments and contribute in a significant way to the ensemble of the flow picture of the Bering Sea.

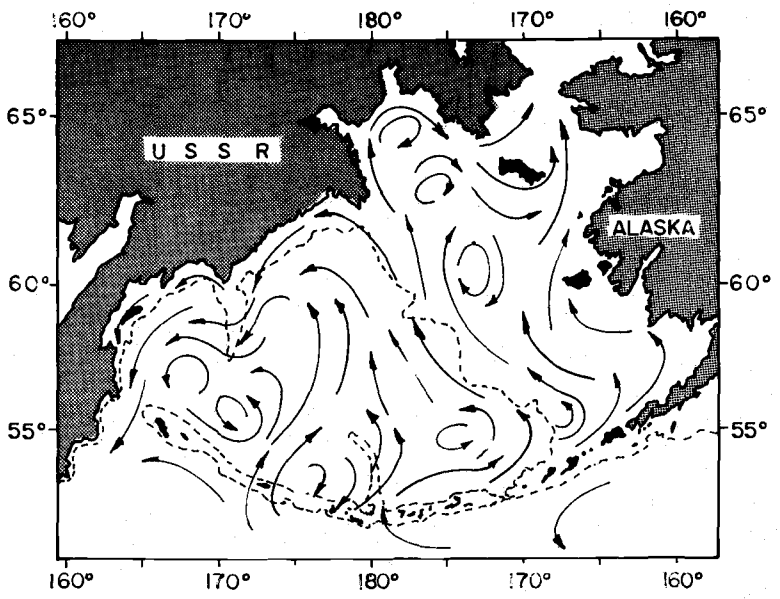


Fig. 13. The Bering Sea circulation according to Arsen'ev (1967).

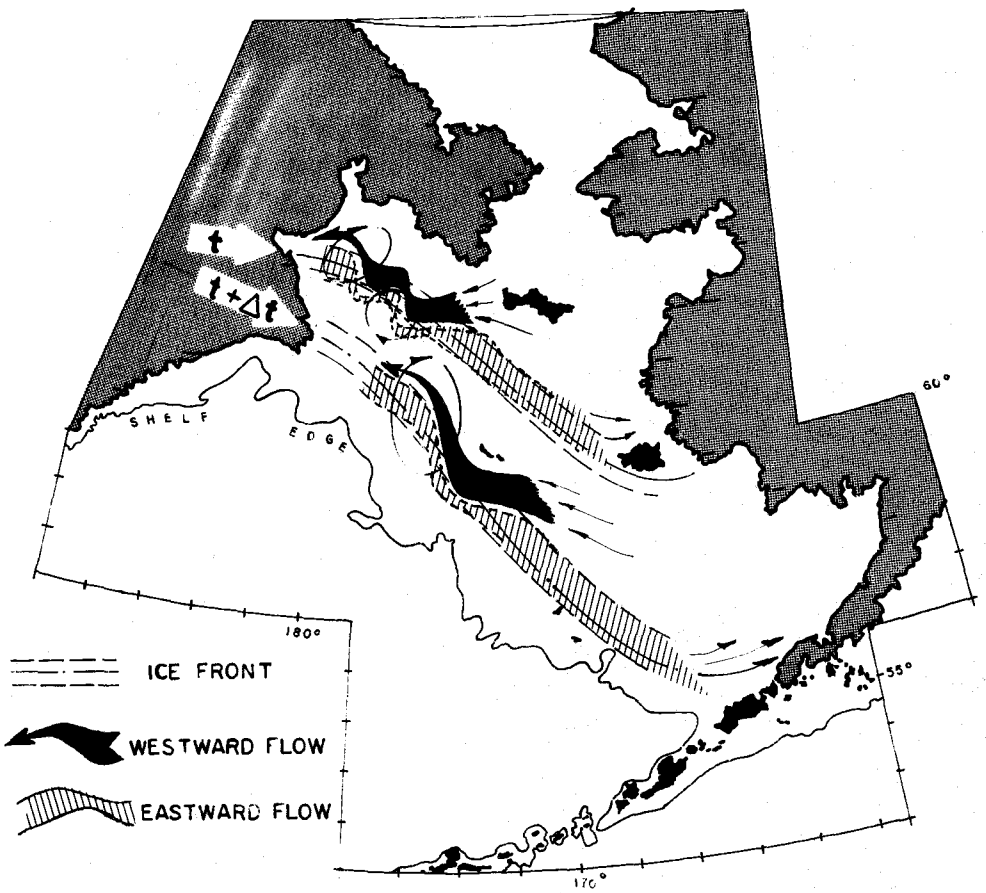


Figure 14. Proposed scheme of ice front interaction with the existing circulation in the Bering Sea at two given points in time, t and $\Delta t$.

# VI. EPILOGUE

A hypothesis on the possible impact of sea ice formation processes on the dynamics of a shallow marginal polar has been posed and examined. It is clear from the development and discussions presented in this thesis that the impact of the mentioned processes in such regions where a winter pycnocline is absent is an important one, and that it results in an appreciable mass transport over the season of ice formation. It has been shown that an advancing ice front, which is the common way a shallow sea freezes at the beginning of the winter, causes a transport which is independent of the width of the freezing zone, but is directly proportional to the depth of convective mixing the amount of ice formed and the excluded salts. This has been expressed in terms of the change of potential energy of the water column. The assumptions on which the models are based have been shown to be reasonable and therefore the results are considered valid in respect to their direct application to a real situation, and should be measurable.

Based on the above it is here considered that a test of these models is in order. For this purpose it is felt that the Bering Sea shelf is a proper site, through the installation of current-temperature meter arrays in late fall, for their recovery the following year. The disposition of these moorings with subsurface flotation along the 170°

meridian, from 62° to 58 °N, at intervals of 1° of latitude, would permit the cross correlations of the eastward velocity components of successive meter pairs and a comparison of these to the ice front progradation as revealed by ERTS satellite reconnaissance photographs.

It is also proposed that numerical models of the winter circulation of the test site be made, taking into account the induced circulation by the processes here exposed. Doing so should reveal important results in connection with unexplained physical and biological processes.

# BIBLIOGRAPHY

Arsen'ev, V. S. 1967. Techeniya i vodnye massy Beringova morya. (The Currents and Water Masses of the Bering Sea). Izdatel' stvo "Nauka", Moskow. 135 pp.

Cameron, W. M. 1974. Some Dynamic and Budgetary Implications of Circulation Schemes for the Bering Sea. In Oceanography of the Bering Sea: proceedings of an International Symposium. University of Alaska, Fairbanks.

Defant, A. 1961. Physical Oceanography. Pergamon, New York. 2 vols.

Doherty, B. T. and D. R. Kester. 1974. Freezing Point of Seawater. J. of Mar. Res. 32, (2).

Duedall, I. W. 1966. The partial Equivalent Volumes of Salts in Seawater. M.S. Thesis, Oregon State University, Corvallis, Oregon.

Favorite, F. 1974. Flow into the Bering Sea through Aleutian Island Passes. In Oceanography of the Bering Sea: proceedings of an International Symposium. University of Alaska, Fairbanks.

Foldvik, A. and T. Kvinge. 1974. Conditional Instability of Sea Water at the Freezing Point. Deep-Sea Res. 21, pp. 169 to 174.

Foster, T. D. 1968. Haline Convection Induced by the Freezing of Sea Water. Journal of Geophysical Research 73(6), 1933-1938.

Fujino, K., E. L. Lewis and R. G. Perkin. 1974. The Freezing Point of Seawater at Pressures up to 100 Bars. J. Geophys. Res. 79(12), 1792.

Gershanovitch, D. E., N. S. Fadeev, T. G. Liubimova, P. A. Moiseev and V. V. Natarov. 1974. Principal Results of Soviet Oceanographic Investigations in the Bering Sea. In Oceanography of the Bering Sea: proceedings of an International Symposium. University of Alaska, Fairbanks.

Hughes, F. W., L. K. Coachman and K. Aagaard. 1974. Circulation, Transport and Water Exchange in the Western Bering Sea. In Oceanography of the Bering Sea: proceedings of an International Symposium. University of Alaska, Fairbanks.

Kester, D. R. 1974. Comparison of Recent Seawater Freezing Point Data. J. of Geophys. Res. In press.

Kolesnikov, A. G. 1958. On the Growth Rate of Sea Ice. Arctic Sea Ice.

Kraus, E. B. and J. S. Turner. 1967. A One-dimensional Model of the Seasonal Thermocline II. The General Theory and Its Consequences. Tellus 19, 98.

Lake, R. A. and E. L. Lewis. 1972. The Microclimate Beneath Growing Sea Ice. Sea Ice Conference Proceedings, Reykjavik.

Lewis, E. L. and E. R. Walker. 1970. The Water Structure under a Growing Ice Sheet. J. of Geophys. Res. 75(33), 6836.

Lewis, E. L. 1973. Convection Beneath Sea Ice. Colloques Internationaux du C.N.R.S. N° 215. Processus de Formation des Eaux Profondes.

Lyman, J. and R. H. Fleming. 1940. Composition of Seawater. Jour. Mar. Res., 3, 134-146.

Maykut, G. and N. Untersteiner. 1971. Some Results from a Time-Dependent Thermodynamic Model of Sea Ice. J. Geophys. Res. 76(6), 1550.

Neumann, G. and W. Pierson. 1966. Principles of Physical Oceanography. Prentice-Hall, Inc., p. 130.

Pounder, E. R. 1962. The Physics of Sea Ice. In The Sea, Vol. 1. John Wiley and Sons. p. 826.

Simpson, L. S. 1958. Estimation of Sea Ice Formation and Growth. Arctic Sea Ice.

Solomon, H. 1969. Large Scale Response of the Ocean to Sea Ice Formation. Ph. D. Thesis, Massachusetts Institute of Technology, Cambridge, Mass.

Sverdrup, H. U., M. W. Johnson and R. H. Fleming. 1942. The Oceans. Prentice-Hall, Inc. 1087 pp.

Tabata, T. 1958. On the Formation and Growth of Sea Ice Especially on the Okhotsk Sea. Arctic Sea Ice.

Takenouti, A. Y. and K. Ohtani. 1974. Currents and Water Masses in the Bering Sea: A Review of Japanese Work. In Oceanography of the Bering Sea: proceedings of an International Symposium. University of Alaska, Fairbanks.

Zubov, N. N. 1943. Arctic Ice. Translation by the United States Naval Oceanographic Office and the American Meteorological Society, published by the United States Navy Electronics Laboratory, San Diego, 491 pp.